Published Ahead of Print on May 21, 2020, as doi:10.3324/haematol.2019.226852.

haematologica
Journal of The Ferrata Storti Foundation

2'-O-methoxyethyl splice-switching oligos correct splicing from IVS2-745 β-thalassemia patient cells restoring HbA production and chain rebalance

by Alisa Dong, Valentina Ghiaccio, Irene Motta, Shuling Guo, Raechel Peralta, Susan M. Freier, Andy Watt, Sagar Damle, Yasuhiro Ikawa, Danuta Jarocha, Maxwell Chappell, Coralea Stephanou, Paola Delbini, Connie Chen, Soteroula Christou, Marina Kleanthous, Kim Smith-Whitley, Deepa Manwani, Carla Casu, Osheiza Abdulmalik, Maria Domenica Cappellini, Stefano Rivella, and Laura Breda

Haematologica 2020 [Epub ahead of print]

Citation: Alisa Dong, Valentina Ghiaccio, Irene Motta, Shuling Guo, Raechel Peralta, Susan M. Freier, Andy Watt, Sagar Damle, Yasuhiro Ikawa, Danuta Jarocha, Maxwell Chappell, Coralea Stephanou, Paola Delbini, Connie Chen, Soteroula Christou, Marina Kleanthous, Kim Smith-Whitley, Deepa Manwani, Carla Casu, Osheiza Abdulmalik, Maria Domenica Cappellini, Stefano Rivella, and Laura Breda. 2'-O-methoxyethyl splice-switching oligos correct splicing from IVS2-745 β-thalassemia patient cells restoring HbA production and chain rebalance. Haematologica. 2020; 105:xxx doi:10.3324/haematol.2019.226852

2'-O-methoxyethyl splice-switching oligos correct splicing from IVS2-745 β-thalassemia patient cells restoring HbA production and chain rebalance

Alisa Dong[1,2*], Valentina Ghiaccio[1*], Irene Motta[3], Shuling Guo[4], Raechel Peralta[4], Susan M. Freier[4], Andy Watt[4], Sagar Damle[4], Yasuhiro Ikawa[1], Danuta Jarocha[1], Maxwell Chappell[1], Coralea Stephanou[5], Paola Delbini[3], Connie Chen[2], Soteroula Christou[5], Marina Kleanthous[5], Kim Smith-Whitley[1], Deepa Manwani[6], Carla Casu[1], Osheiza Abdulmalik[1], Maria Domenica Cappellini[3], Stefano Rivella[1] and Laura Breda[1°]

* These authors contributed equally to this work
° Corresponding author

[1] Division of Hematology, Department of Pediatrics, The Children's Hospital of Philadelphia, Philadelphia, 19104, PA
[2] Graduate School of Medical Sciences, Weill Cornell Medical College of Cornell University, New York, NY, 10021, USA
[3] University of Milan - Fondazione IRCCS Ca' Granda Ospedale Policlinico, Milan, 20122, Italy
[4] Ionis Pharmaceuticals, Carlsbad, CA, 92010, USA
[5] Molecular Genetics Thalassaemia Department, The Cyprus Institute of Neurology and Genetics, 2370 Nicosia, Cyprus
[6] The Children's Hospital at Montefiore, Bronx, NY, 10467, USA

Abstract

β-thalassemia is a disorder caused by altered hemoglobin protein synthesis and affects individuals worldwide. Severe forms of the disease, left untreated, can result in death before the age of 3 years (1). The standard of care consists of chronic and costly palliative treatment by blood transfusion combined with iron chelation. This dual approach suppresses anemia and reduces iron-related toxicities in patients. Allogeneic bone marrow transplant is an option, but limited by the availability of a highly compatible HSC donor. While gene therapy is been explored in several trials, its use is highly limited to developed regions with centers of excellence and well-established healthcare systems (2). Hence, there remains a tremendous unmet medical need to develop alternative treatment strategies for β-thalassemia (3).
Occurrence of aberrant splicing is one of the processes that affects β-globin synthesis in β-thalassemia. The (C>G) IVS2-745 is a splicing mutation within intron 2 of the β-globin gene. It leads to an aberrantly spliced mRNA that incorporates an intron fragment. This results in an in-frame premature termination codon that inhibits β-globin production.

Here, we propose the use of uniform 2'-O-methoxyethyl (2'-MOE) splice switching oligos (SSOs) to reverse this aberrant splicing in the pre-mRNA. With these SSOs we show aberrant to wild type splice switching. This switching leads to an increase of adult hemoglobin (HbA) up to 80% in erythroid cells from patients with the IVS2-745 mutation. Furthermore, we demonstrate a restoration of the balance between β-like- and α-globin chains, and up to an 87% reduction in toxic α-heme aggregates. While examining the potential benefit of 2'-MOE-SSOs in a mixed sickle-thalassemic phenotypic setting, we found reduced sickle hemoglobin (HbS) synthesis and

sickle cell formation due to HbA induction. In summary, 2'-MOE-SSOs are a promising therapy for forms of β-thalassemia caused by mutations leading to aberrant splicing.

Introduction

β-thalassemia is caused by inheritance of one or more of over 400 different mutations in the β-globin gene, which results in reduced (β+ allele) or absent (β0 allele) synthesis of the β-globin chains. The severity of β-thalassemia correlates to the level of imbalance between α- and β-like globin chains. The excess α-globin content in erythroid cells combine to form insoluble hemichromes that damage cell membranes, while their heme component leads to the formation of toxic reactive oxygen species (ROS) and increased oxidative stress. In combination, these factors result in ineffective erythropoiesis and apoptosis in the erythroid lineage (4, 5).
Some β-thalassemia mutations create new cryptic splice sites and, even though the original splice sites are intact, impair normal splicing. Such mutations activate aberrant splice sites and change the splicing pathway (6).

The IVS2-745 mutation creates an aberrant 5' splice site at nucleotide 745 of intron 2 and activates a common cryptic 3' splice site at nucleotide 579 within the same intron (Supplementary Figure 1). Portions of the intronic sequence between the newly activated splice sites are recognized by the splicing machinery as exons and are incorrectly retained in the spliced mRNA. The retained intronic sequence of 165nt carries a stop codon that prevents proper translation of the mRNA and causes a deficiency in β□globin leading to β□thalassemia (7). The IVS2-745 is a β+ allele, whose correct splice sites remain potentially functional and produce a significantly reduced amount of correctly spliced β-globin mRNA and consequently HbA (8). Despite the fact that some HbA is made, in homozygosity, the IVS2-745 mutation leads to severe transfusion-dependent thalassemia major (Hb VAR database: https://globin.bx.psu.edu/hbvar/menu.html).

Since defective β□globin genes like IVS2-745 preserve correct splice sites, approaches based on interference between the spliceosome machinery and the aberrant splice site interaction, have been developed and successfully shown to restore the normal β-globin splicing pattern (9).
The 2'-O-methoxyethyl modification (2'-MOE) chemistry is currently the most advanced of the 2'-modified series of antisense oligonucleotides. Uniformly distributed 2'-MOE-SSOs are not subject to RNase H degradation when they bind their targets, which may be due to the steric hindrance conferred throughout the oligo by the methoxyethyl group (10, 11). Over thirty 2'-MOE based compounds are currently being tested in clinical trials for cancer and cardiovascular, metabolic, and neurological diseases through assessment of safety, tolerability and pharmacokinetics (12, 13). Safety studies of 2'-MOE SSOs show they are well tolerated in multiple species from rodents to non-human primates (14, 15). Thus, they make an attractive candidate for clinical applications, including at least one approved treatment and multiple ongoing clinical trials (16-19).

Here, we demonstrate that uniform 2'-MOE-SSOs targeting the IVS2-745 mutation are effective in treating erythroid cells from thalassemic patients. The 2'-MOE-SSOs exert physical obstruction on the alternative splicing site, preventing recognition from the spliceosome (20) and favoring the correct splicing of the pre-mRNA. By preventing incorrect splicing and therefore avoiding alternative splicing patterns of pre-mRNA, 2'-MOE-SSOs increase HbA production.

Furthermore, 2'-MOE-SSOs alleviate other previously unstudied thalassemic cell parameters, such as a recovery of the stoichiometry of α and β globin chains, a reduction of toxic α aggregates, and the correction of erythrocyte deformities in cells derived from patients heterozygous for the IVS2-745 and sickle cell anemia mutation.

Methods

Human Ethics

Patients were recruited and samples obtained according to the Declaration of Helsinki, following approvals by the (A) Institutional Ethics Committee of the Fondazione Istituto di Ricovero e Cura a Carattere Scientifico Ca' Granda Ospedale Maggiore Policlinico, Milan, #391/2012 for P1, P2, and P4 (B) Cyprus National Bioethics Committee, National Grant ΕΕΒΚ/ΕΠ/2012/05, E.U. Grant ΕΕΒΚ/ΕΠ/2013/23 for P3 and P5 and (C) Children's Hospital of Philadelphia, Institutional Review Board (IRB) #15-012123 for S1. S2 was obtained during automated red cell exchange as part of routine clinical care; as S2 was unlinked and de-identified medical waste, the Montefiore Medical Center IRB deemed it IRB-exempt. All subjects gave their informed consent prior to their inclusion in the study.

Human Erythroblast Culture and Treatment

Whole blood underwent CD34+ selection using immunomagnetic separation (Miltenyi Biotec). CD34+ cells were kept undifferentiated in expansion media with bi- or tri-weekly media changes at a cell density <0.5e6 cells/mL. After 12 days in expansion, cells were transferred into differentiation media.

2'-MOE-SSO treatment via syringe loading occurred on day 14. Cells were resuspended at a concentration of 1e6/100μL in a solution with the 2'-MOE-SSO (at a starting dose of 5 μM) and were passed 10 times through a 25 gauge needle (21), followed by a 1 hour incubation at 37ºC. Following 2'-MOE-SSO treatment, cells were plated at 1e6 cells/mL in fresh differentiation media.

Transduction with lentiviral vectors (AnkCT9W or AnkCT9W-745) were performed within the expansion phase (around day 10) at low MOI (<10) to reach low integration rate (below 3 copies). After transduction, cells were seeded for a few more days in fresh expansion media. Both transduced or 2'-MOE-SSO treated cells were put in differentiation media for up to 6 days. Vector copy number (VCN) in transduced cells was determined by Q-PCR (see supplementary methods). Toxicity was assessed by trypan blue staining (22) and level of differentiation was assessed by benzidine staining (23).

Media for CD34+cells and erythroid culture

CD34+ expansion media: serum-free StemSpan supplemented with: 10μL/mL CC-100 (both Stemcell Technologies), 2 U/mL Erythropoietin (Amgen), 10^{-6} M dexamethasone (Sigma) and 100 U/ml penicillin/streptomycin (GIBCO, ThermoFisher Scientific). Differentiation media: Iscove's Modified DMEM (Cellgro) with 3% AB serum (Atlanta Biologicals), 2% Human Plasma (Stemcell Tech), 10ug/mL Insulin (Sigma), 3U/mL Heparin, 200ug/mL Transferrin (Athens Research & Technology), 10ng/mL SCF (Peprotech), 3U/mL Erythropoietin. Freeze Media: 50% characterized FBS (Hyclone), 10% DMSO (Sigma), and 40% Iscove's Modified DMEM. Thaw Media: Iscove's Modified DMEM supplemented with 5% characterized FBS.

Globins single-chain and tetrameric Hb analysis by direct- and reverse-phase high performance liquid chromatography (HPLC)

Cell pellets were disrupted with Cytobuster (EMD Millipore) for single-chain analysis and with water for tetramer analysis. Single-chain quantification was assessed by reverse-phase HPLC. Hemolysates were injected into a Hitachi D-7000 HSM Series apparatus (Hitachi Instruments) using a Zorbax 5 µm 300SB-C8 300 Å, LC 150 x 2.1 mm column (Agilent Technologies) and a gradient from 20% to 60% acetonitrile in 0.1% trifluoroacetic acid in 25 minutes, with UV detection at 215 nm. Standards of HbA, fetal hemoglobin (HbF), HbS, and hemoglobin C (HbC) were injected (Analytical Control Systems) and used to determine various hemoglobin peak types (23). For tetrameric analysis hemolysates were loaded into a System Gold 126 Solvent Module instrument (Beckman Coulter). Hemoglobin tetramers were separated on a weak cation-exchange PolyCAT A column (PolyLC), and detected at a wavelength of 415 nm. Hb were bound to the column with mobile phase A (20 mmol/L Bis-Tris, 2 mmol/L KCN, pH 6.96) and eluted with mobile phase B (20 mmoI/L Bis-Tris, 2 mmol/L KCN, 200mmol/L NaCl, pH 6.55).

In vitro RBC sickling and morphological analysis

Treatment with 50 µM of either scramble or 91 2'-MOE-SSO occurred 2-3 days after start of differentiation. Cells were then cultured for 6 days in differentiation media before harvest. We assessed the degree of cell sickling in specimens under hypoxic conditions, using previously reported methodology (24, 25). Briefly, 0.5-1 million cells were suspended in isotonic Hemox buffer (TCS Scientific Corp), pH 7.4, supplemented with 10 mM glucose and 0.2% bovine serum albumin, in individual wells of a Costar polystyrene 96-well microplate (Corning). The microplate was then transferred to a Thermomixer R shaker-incubator (Eppendorf), and maintained under hypoxia (Nitrogen gas), with continuous agitation at 500 rpm, at 37° C for 2 hours. At conclusion, aliquots of each sample were collected in 2% glutaraldehyde solution for immediate fixation without exposure to air. Subsequently, fixed cell suspensions were introduced into specialized glass microslides (Dawn Scientific) for acquisition of bright field images (at 40x magnification) of single layer cells on an Olympus BX40 microscope fitted with an Infinity Lite B camera (Olympus) and the coupled Image Capture software.

Results

2'-MOE-SSOs induce splice switching, restoring adult hemoglobin (HbA) production in cells from patients with β0/IVS2-745 genotype.

In order to find the most efficacious oligonucleotides to block the aberrant splicing caused by the C>G mutation in IVS2-745, we designed SSOs spanning the 165bp extra exon and the regions upstream and downstream of this exon. All the SSOs are 18-mer oligonucleotides with uniform 2'-MOE modifications of each nucleoside sugar moiety, referred to herein as “2'-MOE-SSOs”. These 2'-MOE-SSOs were screened in mouse erythroleukemia (MEL) cells expressing the aberrant IVS2-745 HBB for splicing correction (Supplementary Figure 2). The top 3 2'-MOE-SSOs, hereinafter referred to by identification numbers, 91, 92, 93, showed the most effective increase of wildtype HBB mRNA expression and were selected for further investigation. These 2'-MOE-SSOs cluster in the 5'-end of the extra exon, within 50 nucleotides of the 3'-cryptic splicing site. A 2'-MOE-SSO not targeting any region was used as a scrambled control to evaluate any potential non-sequence specific effect. The sequences of the oligonucleotides and their binding sites on the β-globin gene are provided in Supplementary Tables 2 and 3,

respectively. The binding areas of the three 2'-MOE-SSOs and the predicted splicing factor binding sites, obtained through a search of the RNA-binding Protein DataBase (RBPDB) at http://rbpdb.ccbr.utoronto.ca, have been provided in Supplementary Table 4.

We isolated hematopoietic stem cells (HSCs) from peripheral blood mononuclear cells from patients' blood using immunobeading (25). HSCs were subsequently expanded and differentiated using a two-phase liquid culture system adapted from a previously described (26) and its formulation is summarized in the methods section. After two days of differentiation the 2'-MOE-SSOs treatment occurred by syringe loading. The differentiated erythroblasts were collected at the conclusion of cell culture. Characterization of differentiating WT cells and β-thalassemic (BT) cells, with one allele affected by IVS2-745 mutation in combination with an IVS1-6 allele, at day 2, 5 and 8 by benzidine staining and flow cytometry of the CD71, CD235a (GPA) along with other markers is depicted in Supplementary Figure 3. While surface markers seem unaffected in WT and BT specimen, total HbA proportion and concentration per cell is diminished in the BT specimen, as well as the amount of WT HBB mRNA, as shown in Supplementary Figure 4. This reiterates the concept that the defect in BT cells is a quantitative one, completely dependent on the reduced level of β-globin gene expression and translation. Following treatment, we detected corrected splice reversal in differentiated IVS2-745/β0 erythroblasts at a dose as low as 5 μM of the IVS2-745 specific 2'-MOE-SSOs. As expected, the samples treated with scramble 2'-MOE-SSO exhibited alternative splicing: both the longer 745 aberrant and the shorter WT mRNA forms were detected by electrophoresis (Supplementary Figure 5).

Amplicons of both WT and aberrant IVS2-745 cDNA forms were extracted, purified and subcloned. The sequence of the amplicons subcloned matched the aberrant mRNA sequence with the extra 165bp intronic segment retained after aberrant splicing of the IVS2-745 allele, which was not present in the correctly spliced β-globin mRNA band (Supplemental Table 1). While both 2'-MOE-SSOs 92 and 93 were effective, the most robust effect was observed in specimens treated with 2'-MOE-SSO 91. We tested 2'-MOE-SSOs concentration in steps and according to specimens' accrual. The first attempted treatment with the 5μM dose (Supplementary Figure 5A) showed a strong reduction of the aberrant IVS2-745 alternative splice variant in specimen P1.

As patient sample collection requires both access to donors and trained researchers to isolate HSCs, we escalated the dose in subsequent patient samples. Accordingly, P2 was then treated with an 25μM dose, which decreased the aberrant mRNA form further, indicating a dose-dependent response to the 2'-MOE-SSOs (Supplementary Figure 5A). Given the high cell viability observed at 25uM, all further specimens were treated increasing the dose to 50μM (Supplementary Figure 5C and D). At this dose amplification of the aberrant IVS2-745 splicing is nearly undetected, while it remains unaltered in the specimens treated with the scramble 2'-MOE-SSO. The strong WT signal in untreated or scramble-treated specimens is likely due to the higher stability of the WT compared to the aberrant mRNA form (27) and further justified by the nature of the RT-PCR assay, which is a semi-quantitative method and does not necessarily reflect the absolute content of the two species in the samples. These results were obtained without cell loss, as previously reported in other studies based on the use of 2'-MOE-SSOs (28).

We observed no statistical difference in viability or cell differentiation in the majority of treatments at the aforementioned treatment dosages (Figure 1).

Despite the presence of detectable levels of WT β-globin mRNA, the amount of HbA measured by HPLC was relatively low in untreated specimens (Figure 2A). Upon 2'-MOE-SSO treatment, HbA levels were increased and a significant reduction of α-heme aggregates was observed. Once again, treatment with 2'-MOE-SSO 91 induced the most robust outcome. At the 5 μM dose, 2'-MOE-SSO 91 induced HbA increase from baseline levels of 2.60 ± 0.17% and 4.65 ± 0.46% to 29.21± 2.16% and 27.94 ± 1.09%, in specimens P1 and P2, respectively. At the 50 μM dose, 2'-MOE-SSO 91 induced an HbA increase from baseline levels of 4.20 ± 0.75% and 2.97 ± 0.23% HbA to 59.14 ± 1.34% and 60.21 ± 2.61%, in specimens P3 and P4, respectively, indicating a corresponding 15- and 20-fold increase in HbA. Q-PCR analyses of the messenger RNA obtained from the same specimens show a similar trend (Figure 2B). In these, the amount of correctly spliced WT β-globin mRNA increased up to 100-fold, relative to baseline levels, at the 50 μM dose of 2'-MOE-SSO 91.

The baseline α-heme aggregate (26) level in heterozygous cells was variable across samples, with means ranging from 4.28 ± 1.12%, in P4, to 22.00 ± 0.76%, in P1 (Figures 3A, 3B). We detected a significant reduction in aggregates across all 2'-MOE-SSO treatments, more pronounced for 2'-MOE-SSO 91 (Figure 3C), in specimen P1, with up to 54% decrease. In specimen P2, a significant reduction in aggregates was seen starting at a 25 μM dose. Although baseline levels of α-heme aggregates in P3 and P4 were lower, 2'-MOE-SSOs 91 and 93 still elicited a significant α-heme aggregate reduction at a 50 μM dose. Consistent with our previous observations, 2'-MOE-SSO 91 was the most effective, with as high as an 87% reduction in α-heme aggregates (specimen P3).

We further compared the potency of 2'-MOE-SSO treatment to the effect of a lentiviral vector, AnkCT9W, carrying a WT copy of the β-globin gene in IVS2-745/β0 heterozygous specimens (P1). At an average vector copy number (VCN) of 1.13, erythroblasts transduced with this vector induced an increase of HbA to 50% (Figure 4), which compared to the effect obtained using 2'-MOE-SSO 91 at the concentration of 50μM. This indicates that the 2'-MOE-SSO dose used for our assessment can generate an effect that is comparable to that of a safe single copy gene addition approach.

2'-MOE-SSOs show the most robust effects on cells from homozygous patients with an IVS2-745/IVS2-745 genotype

After demonstrating a dose-dependency in response to 2'-MOE-SSO treatment, we next sought to determine if there was an "allele dose-dependency", e.g., we investigated whether treatment with 2'-MOE-SSOs had a higher impact on a homozygotic sample with two 745 target alleles, compared to a heterozygotic sample, with only one 745 target allele. A homozygotic sample produces exclusively 745 mutant pre-mRNA from both alleles, and thus there could be a 2-fold increase of 745 pre-mRNA target substrate for the 2'-MOE-SSOs to induce normal splice switch than in the case of a single 745 allele. In an additional specimen (P5), homozygous for the IVS2-745 mutation, the ratio of aberrant to WT mRNA detected by RT-PCR was roughly 50:50 (Figure 5A). In this sample, the baseline level of HbA, although low (6.75 ± 0.22%), was slightly

higher than in any of the heterozygous specimens, most likely due to the additive contribution of the endogenous WT spliced mRNA from the two IVS2-745 β+ alleles. As hypothesized, specimen P5 showed the most striking results after treatment with 2'-MOE-SSOs. The IVS2-745 mutant form was almost undetectable by electrophoresis in all treatments (Figure 5A); and there was a 300 to 700-fold increase in correctly spliced WT mRNA in the samples treated with 2'-MOE-SSO 91 (Figure 5B). All three 2'-MOE-SSOs had the highest effect in this homozygotic sample. 2'-MOE-SSO 91 raised HbA levels to 79.46 ± 0.94%, at a 50 μM dose. The 100 μM dose produced similar results (77.92 ± 1.04% HbA), indicating that the effect of this 2'-MOE-SSO reaches a protein plateau at the 50μM dose. 2'-MOE-SSO 92 and 93 raised HbA levels to HbA 71.42 ± 1.22% and 58.48 ± 0.32%, respectively, at the 50μM dose (Figure 5C). The 100 μM 2'-MOE-SSO 91 dose in the homozygote led to a 60% reduction in α-heme aggregates (not shown). While at this dose the effect on the protein production plateaued, Q-PCR data show that the effect of these 2'-MOE-SSOs dramatically increases at 25μM dose, and continue to escalate up to the maximum dose of 100μM (Figure 5B).

In order to examine the effects of 2'-MOE-SSOs treatment on the α:β globin stoichiometry, cell lysates obtained from erythroblasts were analyzed by reverse-phase HPLC. This allowed discrimination of the α chains from the β-like chains (β, γ, δ). Without treatment, the ratio of α:β-like chains ranged from 65:35 in P1 to 55:45, in P4 and P5, respectively, and was significantly different from a healthy control, which showed the expected 50:50 α:β globin stoichiometry (Figure 6). Single-chain separation showed that at a dose as low as a 25 μM, 2'-MOE-SSO 91 was able to restore the 50:50 balance of α chains to β-like chains. The α:β globin stoichiometry in treated samples was comparable to that of healthy control samples.

Direct quantification of WT β-globin messenger confirms high efficiency of treatment with 2'-MOE-SSO 91 on IVS2-745 specimens.
Using droplet digital PCR (ddPCR), we further attested the efficiency of 2'-MOE-SSOs treatment mediated splicing correction on both heterozygous and homozygous specimens for the IVS2-745 mutation. We chose the 2'-MOE-SSO 91 at the 50 μM dose because of its higher performance and the plateauing effect on HbA increase observed in previous experiments, based on Figures 5 and 6.

Treatment with 2'-MOE-SSO 91 in P4, derived from a compound heterozygous patient with an β-IVS2-745/β0 genotype, showed a 19.3-fold increase in WT β-globin mRNA, when normalized by β actin expression (Figure 7A), and a 11-fold increase in WT β-globin mRNA, when normalized by the β-IVS2-745 mRNA expression (Supplementary Figure 6). The proportion of WT β-globin increase was more dramatic in cells from a homozygous patient with an IVS2-745/IVS2-745 genotype (Figure 7B). Treatment of specimen P5 with 2'-MOE-SSOs 91 resulted in a >800-fold increase in WT β-globin mRNA. This improvement in the efficiency of treatment with 2'-MOE-SSO 91 confirmed data previously obtained via Q-PCR and HPLC, and showed how the allele dose-dependency is much more evident when detected with a direct quantification method. Using ddPCR we confirmed that untreated and scrambled-treated presented similar levels of WT β-globin expression, indicating that the use of scramble 2'-MOE-SSOs did not alter the splicing of the β-globin gene in our specimens.

2'-MOE-SSOs prevents sickling in samples with an IVS2-745/β-S genotype

Lastly, we investigated the effect of these 2'-MOE-SSOs on cells with the IVS2-745 mutation in combination with the β-sickle allele. There are limited epidemiological studies on the β-sickle/β-thalassemia genotype, however literature indicates their clinical presentation as severe (29). Clinical complications seen in patients with β-sickle/β-thalassemia genotype are mainly due to the large relative quantity of HbS that is present, given the β-thalassemia allele does not produce enough HbA. As we could not obtain a sample with the compound IVS2-745/β-S genotype, we artificially created a model system, by transducing two homozygous sickle specimens (S1 and S2) with an erythroid-specific lentiviral vector, AnkCT9W-745, that carries an IVS2-745 β-globin transgene. We analyzed integration of transduced S1 and S2 cells and detected a VCN of 2.02 and 1.62, respectively, which replicates a somewhat "heterozygotic" state, as the 2 endogenous sickle alleles were matched by roughly two IVS2-745 alleles in each specimen. Upon differentiation and exposure to hypoxia, S1 scramble-treated cells showed prong-like polymers of sickle chains. 2'-MOE-SSO 91 treatment of S1 resulted in an increase in HbA from 8.96 ± 1.88% to 59.82 ± 0.23%, and a decrease in sickle hemoglobin (HbS), from 75.34 ± 2.33% to 30.73 ± 0.32% (Figure 8A). This increase in HbA proportion at the expense of HbS led to a 50% reduction in the sickling effect. Following treatment, cells had a lower propensity to sickle under hypoxic conditions, as indicated by the lower number of yellow arrows in the right panel of Figure 8B. These results show that 2'-MOE-SSOs could be indicated for use in patients with compound heterozygous IVS2-745 /β-sickle genotype to reduce RBC deformities.

Discussion

2'-MOE-SSOs show targeted therapeutic potential for splice mutants of β-thalassemia. They effectively act at the RNA level where the defect occurs, and lead to restoration of WT β-globin synthesis in thalassemic erythroid cells. The increased production of functional β-globin mRNA leads to increased HbA production, a restoration of the balance between α and β chains, and a reduction in α-heme aggregates. Treatment with the 2'-MOE-SSOs in a cell model that reproduces a β-sickle/β-thalassemia genotype also leads to a sufficient HbA increase to reduce formation of sickle cells under hypoxia.

The increase in WT β-globin expression first shown via RT and Q-PCR was further confirmed using a direct quantification method ddPCR. The amplified effect of treatment with the 2'-MOE-SSOs observed in homozygous, compared to heterozygous treated specimens, reflects an increased targeting of the aberrant spicing generated from two compared to a single IVS2-745 allele. While specimens from patient with an β0/IVS2-745 genotype already show a strong reduction of the aberrant splicing, with consequent increase of HbA to 60%, specimens with IVS2-745 homozygous genotype showed even more dramatic correction upon treatment, showing an increase of HbA to 80%, an amount that could potentially be curative for patients with this genotype.

We observed no significant difference in viability or differentiation for nearly all treatments. Looking toward the future, a side-by-side study would need to be done on multiple patient samples across doses. For our study, the 5 μM and 25 μM dose were used on the same patient and produced no significant differences. However, the 50 μM and 100 μM doses were tested on samples from different patients. As these samples were harvested from different patients, at separate time points, by different collaborators, and shipped separately, we cannot make a true side-by-side comparison. Experiments were limited by the availability of donor material and

skilled researchers to collect it. Better access to local patient databases or training more collaborators could allow such a large-scale study for more comprehensive comparisons.

A barrier to clinical translation is the ability to target the 2'-MOE-SSOs to the bone marrow. 2'-MOE-SSOs need physical or chemical manipulation to enter cultured cells. However *in vivo* and in some primary cell cultures, studies show natural cellular uptake pathways without this manipulation (12). While drug delivery is not in scope for this paper, modulation of splicing has been demonstrated in preclinical models and in the clinic. As a result, two splicing modulation drugs have been approved, Spinraza® for the treatment of spinal muscular atrophy and Eteplirsen for the treatment of Duchenne muscular dystrophy, administered by intrathecal and subcutaneous injections, respectively (16, 17). Upon systemic delivery, antisense oligonucleotides distribute broadly in the tissues, including bone marrow. However, in order to improve the delivery to the cell type of interest, a LICA (ligand conjugated antisense) strategy is needed. GalNAc conjugated ASO improved potency in hepatocytes by about 30 fold in the clinic (30); GLP-1 conjugated ASO LICA strategy has successfully improved the delivery to pancreatic β cells (31). Finding the LICA to specific bone marrow cell types, including CD34+ cells, is an area of active investigation.

In summary, 2'-MOE-SSOs are promising therapeutic tools for certain splicing forms of β-thalassemia. Their ability to correct the underlying splicing defect offers a pharmacological treatment that is both direct and specific. As such, this therapy could help patients reduce their transfusion dependence or even reach transfusion independence. If combined with the appropriate carrier for optimized delivery and absorption, these molecules represent an attractive therapeutic alternative to increase HbA protein in patients with β-thalassemia, without the need for aggressive conditioning regimens and expensive ex-vivo cell manipulation that are mandatory in gene addition and gene editing therapies.

References

1. Modell B, Darlison M. Global epidemiology of haemoglobin disorders and derived service indicators. Bull World Health Organ. 2008;86(6):480-487.
2. Sayani FA, Kwiatkowski JL. Increasing prevalence of thalassemia in America: Implications for primary care. Ann Med. 2015;47(7):592-604.
3. Ghiaccio V, Chappell M, Rivella S, Breda L. Gene Therapy for Beta-Hemoglobinopathies: Milestones, New Therapies and Challenges. Mol Diagn Ther. 2019;23(2):173-186.
4. Camaschella C, Cappellini MD. Thalassemia intermedia. Haematologica. 1995;80(1):58-68.
5. Rivella S. beta-thalassemias: paradigmatic diseases for scientific discoveries and development of innovative therapies. Haematologica. 2015;100(4):418-430.
6. Sierakowska H, Sambade MJ, Agrawal S, Kole R. Repair of thalassemic human beta-globin mRNA in mammalian cells by antisense oligonucleotides. Proc Natl Acad Sci U S A. 1996;93(23):12840-12844.
7. Orkin SH, Kazazian HH, Jr., Antonarakis SE, et al. Linkage of beta-thalassaemia mutations and beta-globin gene polymorphisms with DNA polymorphisms in human beta-globin gene cluster. Nature. 1982;296(5858):627-631.

8. Treisman R, Orkin SH, Maniatis T. Specific transcription and RNA splicing defects in five cloned beta-thalassaemia genes. Nature. 1983;302(5909):591-596.
9. Svasti S, Suwanmanee T, Fucharoen S, et al. RNA repair restores hemoglobin expression in IVS2-654 thalassemic mice. Proc Natl Acad Sci U S A. 2009;106(4):1205-1210.
10. Teplova M, Minasov G, Tereshko V, et al. Crystal structure and improved antisense properties of 2'-O-(2-methoxyethyl)-RNA. Nat Struct Biol. 1999;6(6):535-539.
11. Vickers TA, Wyatt JR, Burckin T, Bennett CF, Freier SM. Fully modified 2' MOE oligonucleotides redirect polyadenylation. Nucleic Acids Res. 2001;29(6):1293-1299.
12. Bennett CF, Swayze EE. RNA targeting therapeutics: molecular mechanisms of antisense oligonucleotides as a therapeutic platform. Annu Rev Pharmacol Toxicol. 2010;50:259-293.
13. Reautschnig P, Vogel P, Stafforst T. The notorious R.N.A. in the spotlight - drug or target for the treatment of disease. RNA Biol. 2017;14(5):651-668.
14. Crooke ST, Baker BF, Kwoh TJ, et al. Integrated Safety Assessment of 2'-O-Methoxyethyl Chimeric Antisense Oligonucleotides in NonHuman Primates and Healthy Human Volunteers. Mol Ther. 2016;24(10):1771-1782.
15. Zanardi TA, Kim TW, Shen L, et al. Chronic Toxicity Assessment of 2'-O-Methoxyethyl Antisense Oligonucleotides in Mice. Nucleic Acid Ther. 2018;28(4):233-241.
16. Finkel RS, Chiriboga CA, Vajsar J, et al. Treatment of infantile-onset spinal muscular atrophy with nusinersen: a phase 2, open-label, dose-escalation study. Lancet. 2016;388(10063):3017-3026.
17. Mendell JR, Goemans N, Lowes LP, et al. Longitudinal effect of eteplirsen versus historical control on ambulation in Duchenne muscular dystrophy. Ann Neurol. 2016;79(2):257-271.
18. Rader DJ, Kastelein JJ. Lomitapide and mipomersen: two first-in-class drugs for reducing low-density lipoprotein cholesterol in patients with homozygous familial hypercholesterolemia. Circulation. 2014;129(9):1022-1032.
19. Ratni H, Mueller L, Ebeling M. Rewriting the (tran)script: Application to spinal muscular atrophy. Prog Med Chem. 2019;58:119-156.
20. Kole R, Williams T, Cohen L. RNA modulation, repair and remodeling by splice switching oligonucleotides. Acta Biochim Pol. 2004;51(2):373-378.
21. Clarke MS, McNeil PL. Syringe loading introduces macromolecules into living mammalian cell cytosol. J Cell Sci. 1992;102(Pt 3):533-541.
22. Strober W. Trypan blue exclusion test of cell viability. Curr Protoc Immunol. 2001;Appendix 3:Appendix 3B.
23. Breda L, Kleinert DA, Casu C, et al. A preclinical approach for gene therapy of beta-thalassemia. Ann N Y Acad Sci. 2010;1202:134-140.
24. Deng W, Rupon JW, Krivega I, et al. Reactivation of developmentally silenced globin genes by forced chromatin looping. Cell. 2014;158(4):849-860.
25. Breda L, Motta I, Lourenco S, Gemmo C, et al. Forced chromatin looping raises fetal hemoglobin in adult sickle cells to higher levels than pharmacologic inducers. Blood. 2016;128(8):1139-1143.
26. Breda L, Casu C, Gardenghi S, et al. Therapeutic hemoglobin levels after gene transfer in beta-thalassemia mice and in hematopoietic cells of beta-thalassemia and sickle cells disease patients. PLoS One. 2012;7(3):e32345.
27. Gemignani F, Sazani P, Morcos P, Kole R. Temperature-dependent splicing of beta-globin pre-mRNA. Nucleic Acids Res. 2002;30(21):4592-4598.

28. Disterer P, Kryczka A, Liu Y, et al. Development of therapeutic splice-switching oligonucleotides. Hum Gene Ther. 2014;25(7):587-598.
29. Gonzalez-Redondo JM, Kutlar F, Kutlar A, et al. Hb S(C)-beta+-thalassaemia: different mutations are associated with different levels of normal Hb A. Br J Haematol. 1988;70(1):85-89.
30. Crooke ST, Baker BF, Xia S, et al. Integrated Assessment of the Clinical Performance of GalNAc3-Conjugated 2'-O-Methoxyethyl Chimeric Antisense Oligonucleotides: I. Human Volunteer Experience. Nucleic Acid Ther. 2019;29(1):16-32.
31. Ammala C, Drury WJ 3rd, Knerr L, et al. Targeted delivery of antisense oligonucleotides to pancreatic beta-cells. Sci Adv. 2018;4(10):eaat3386.

Legend to Figures

Figure 1. Cell viability and differentiation rate in patients' erythroblasts.
(A) Percentage of live/dead cells counted by trypan blue assay. (B) Number of hemoglobinized cells (benzidine-positive count).

Figure 2. 2'-MOE-SSOs induce increase of HbA production and WT β-globin mRNA in IVS2-745/β0 heterozygous sample.
(A) Percentage of HbA from cell lysates as detected by HPLC. (B) Q-PCR for only correctly spliced WT β-globin mRNA. Scale indicates relative expression as normalized to the housekeeping gene GAPDH and red-cell specific gene glycophorin A. n=3. S= scramble treated control at same dose. All statistics (ANOVA/Kruskal-Wallis) are compared to scramble control. **p< 0.01 ***p< 0.001, ****p< 0.0001.

Figure 3. Representative HPLC profile of the separation of hemoglobins in IVS2-745/β0 heterozygous sample treated with 2'-MOE-SSO 91.
(A) Presence of α-heme aggregates and low levels of HbA detected in untreated cells from P1. (B) After treatment with 2'-MOE-SSO 91 the production of adult hemoglobin was increased 11 fold and α-heme aggregates were reduced two fold. Fetal and HbA2 levels were unaltered. (C) Percentage of α-heme aggregates detected by HPLC in treated samples. All statistics (ANOVA/Kruskal-Wallis) are compared to scramble control. *p< 0.1 **p< 0.01 ***p< 0.001, ****p< 0.0001.

Figure 4. Comparison of the efficacy of HbA production between 2'-MOE-SSO 91 and lentiviral transduction in IVS2-745/β0 heterozygous sample.
Percentage of HbA detected by HPLC in control and after treatment. VCN determined via Q-PCR.
All statistical comparisons (ANOVA/Kruskal-Wallis) are tested against scramble control, n=3. NS=not significant, **p< 0.01, **** p< 0.0001.

Figure 5. Additive effect of 2'-MOE-SSOs in homozygous IVS2-745 patient cells (P5).
(A) Electrophoresis of PCR products of cDNA obtained from erythroblasts from specimen P5. WT and IVS2-745 β-globin amplified products are indicated in untreated and treated specimens at the 50μM and 100μM doses. (B) Q-PCR analyses of correctly spliced WT β-globin mRNA.

Values in y axes indicate β-globin expression normalized to the housekeeping GAPDH gene expression and red-cell specific glycophorin A gene expression. (C) Percentage of HbA in scramble-treated control (S) and 2'-MOE-SSO treated specimens (91-92-93) at same dose (n=3). All statistical comparisons (ANOVA/Kruskal-Wallis) are tested against scramble control. **p< 0.01 ***p< 0.001, ****p< 0.0001.

Figure 6. 2'-MOE-SSO 91 restores the balance between α and β globin chains ratio.
Single chain analysis of α chains to β-like chains (β, γ, δ) ratio. All statistical analyses (ANOVA/Kruskal-Wallis) are tested against scramble control. N=3. NS=not significant, **p< 0.01, **** p< 0.0001.

Figure 7. 2'-MOE-SSO 91 greatly increases amounts of WT β-globin mRNA.
In these ddPCR analyses, y axes indicate relative expression of WT β-globin normalized to the housekeeping gene β-actin in (A) IVS2-745/β0 heterozygous sample, P4, and (B) IVS2-745 homozygous sample, P5. In both samples, 2'-MOE-SSO scramble and 2'-MOE-SSO 91 treatment were at the dose of 50μM. All statistical comparisons (ANOVA/Kruskal-Wallis) are tested against scramble-treated and non-treated sample. n=3. *p< 0.1, **p< 0.01, **** p< 0.0001.

Figure 8. 2'-MOE-SSO 91 can rebalance the ratio of hemoglobins and produce enough functional HbA to prevent sickling.
(A) Percentage of HbA, HbS and fetal hemoglobin (HbF) chains detected by HPLC analysis in control-untreated, scramble-treated and oligo 91-treated specimens, at same dose of 50μM, n=3. (B) In vitro sickling assay. IVS2-745/β-S cells were treated with scramble or oligo 91, then exposed to hypoxia. Barbed cells with long polymers of pointy sickle chains are indicated by yellow arrows.

Figure 1

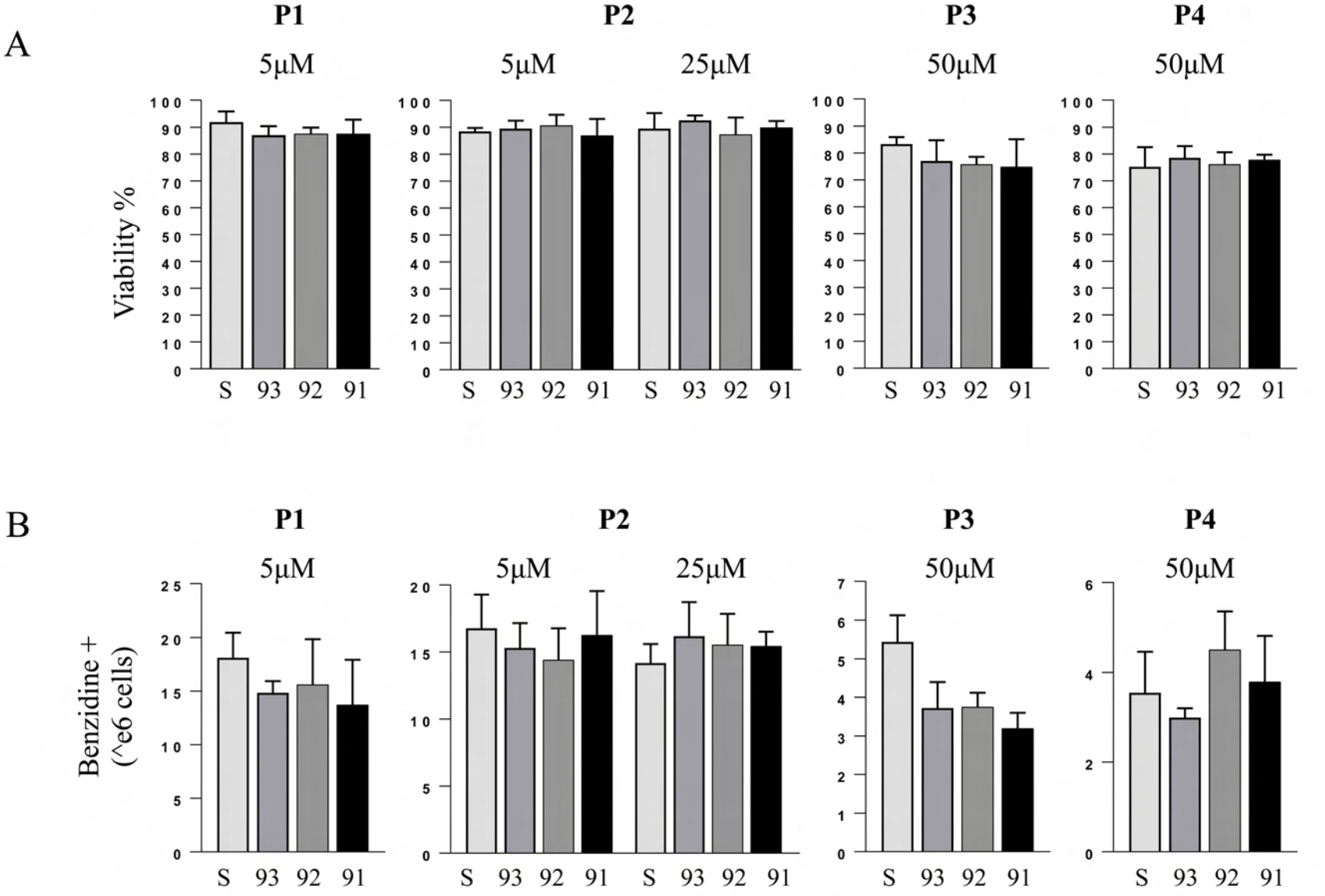
A
P1
5µM
P2
5µM
25µM
P3
50µM
P4
50µM
Viability %
100
90
80
70
60
50
40
30
20
10
0
S
93
92
91
B
P1
5µM
P2
5µM
25µM
P3
50µM
P4
50µM
Benzidine +
(^e6 cells)
25
20
15
10
5
0
7
6
5
4
3
2
1
0
S
93
92
91

Figure 2

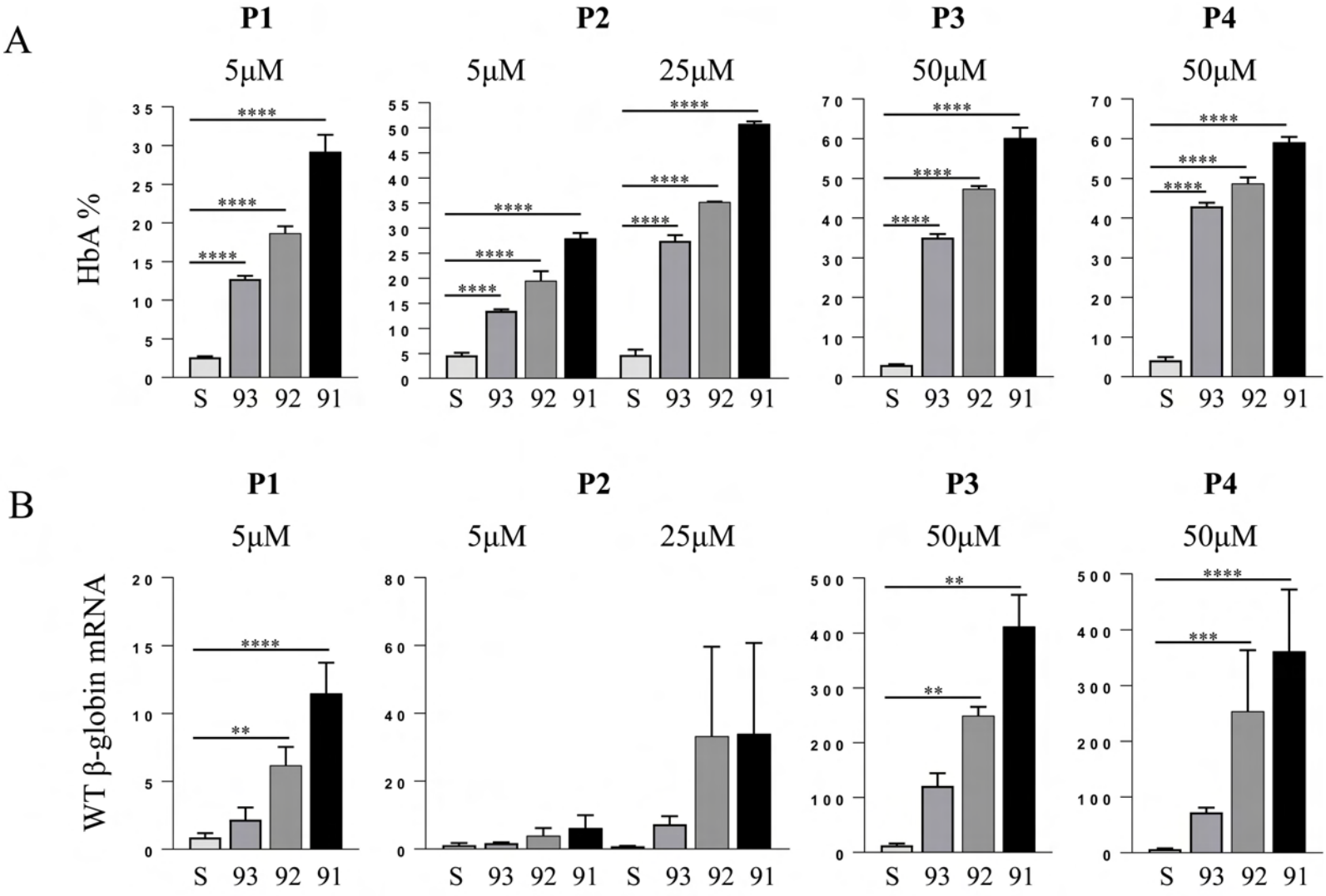
A
P1
5μM
P2
5μM
25μM
P3
50μM
P4
50μM
HbA %
S 93 92 91
****
B
P1
5μM
P2
5μM
25μM
P3
50μM
P4
50μM
WT β-globin mRNA
S 93 92 91
**
***
****

Figure 3

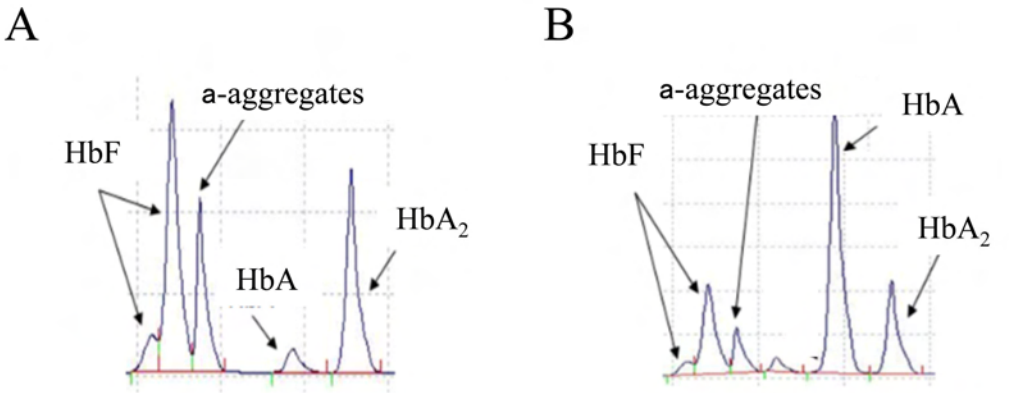
A
a-aggregates
HbF
HbA2
HbA
B
a-aggregates
HbA
HbF
HbA2

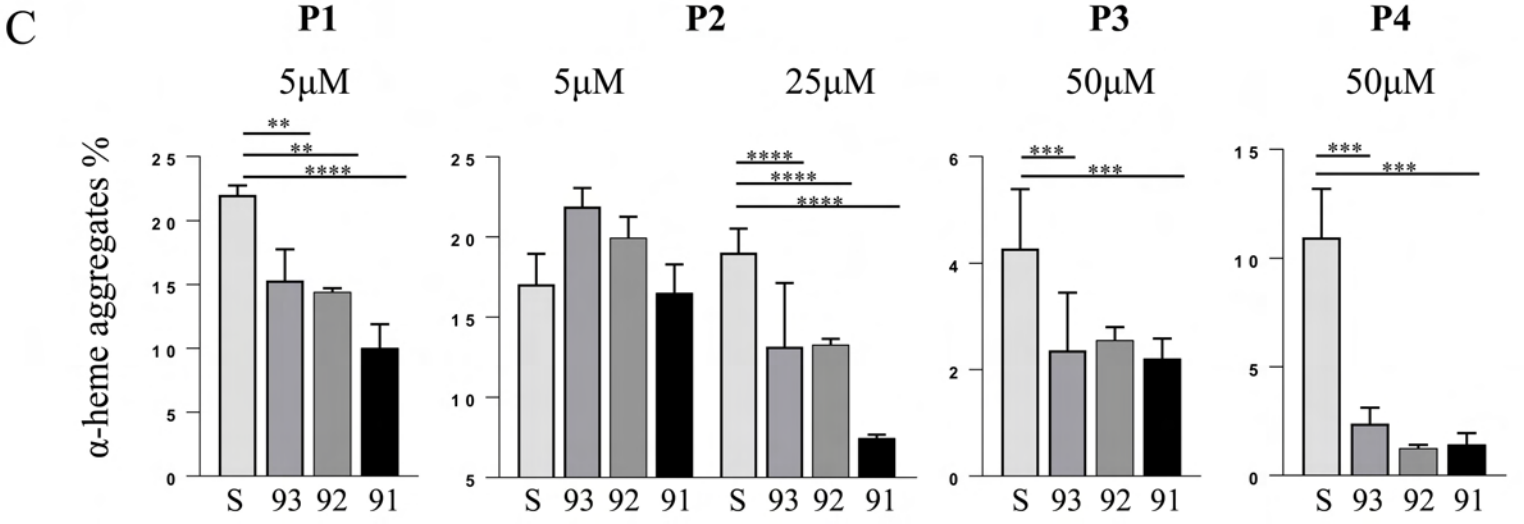
C
P1
5µM
P2
5µM
25µM
P3
50µM
P4
50µM
α-heme aggregates %
S 93 92 91

Figure 4

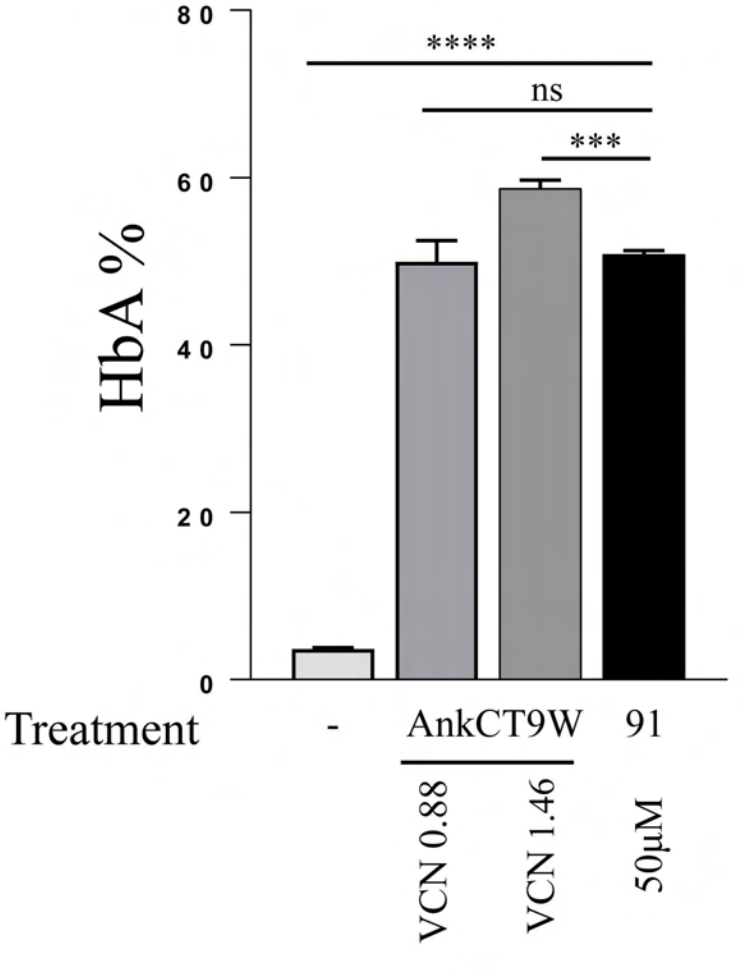

Figure 5

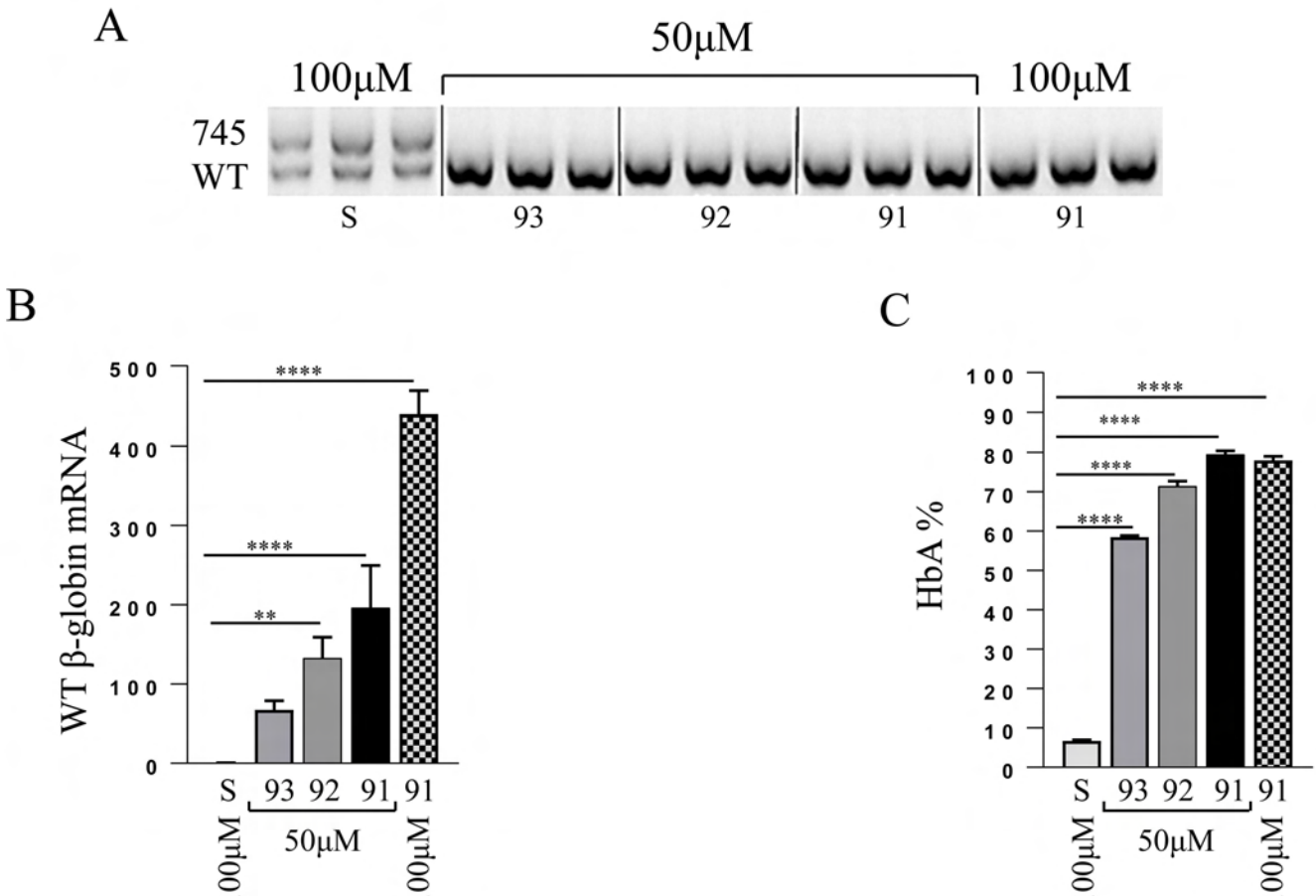
A
100μM
50μM
100μM
745
WT
S
93
92
91
91
B
WT β-globin mRNA
500
400
300
200
100
0
****
****
**
S
93
92
91
91
100μM
50μM
100μM
C
HbA %
100
90
80
70
60
50
40
30
20
10
0
****
****
****
****
S
93
92
91
91
100μM
50μM
100μM

Figure 6

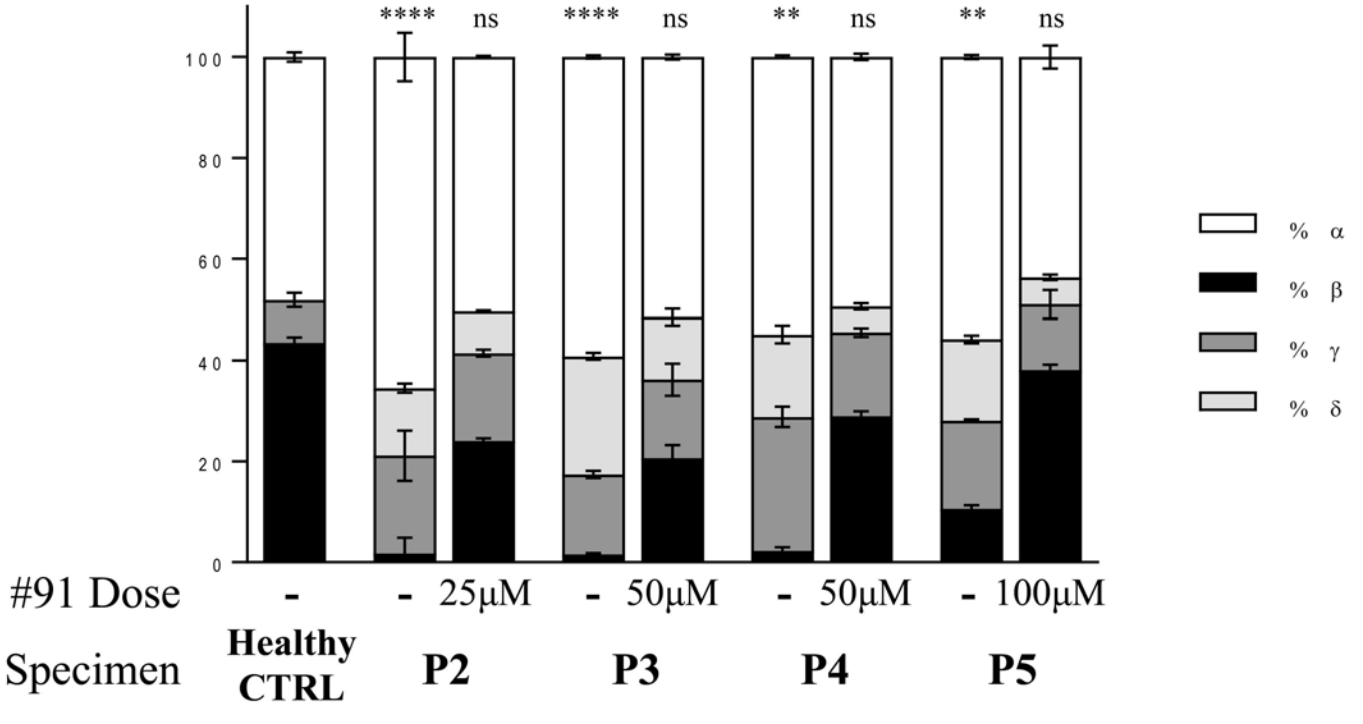
****
ns
****
ns
**
ns
**
ns
100
80
60
40
20
0
% α
% β
% γ
% δ
#91 Dose
-
- 25μM
- 50μM
- 50μM
- 100μM
Specimen
Healthy CTRL
P2
P3
P4
P5

Figure 7

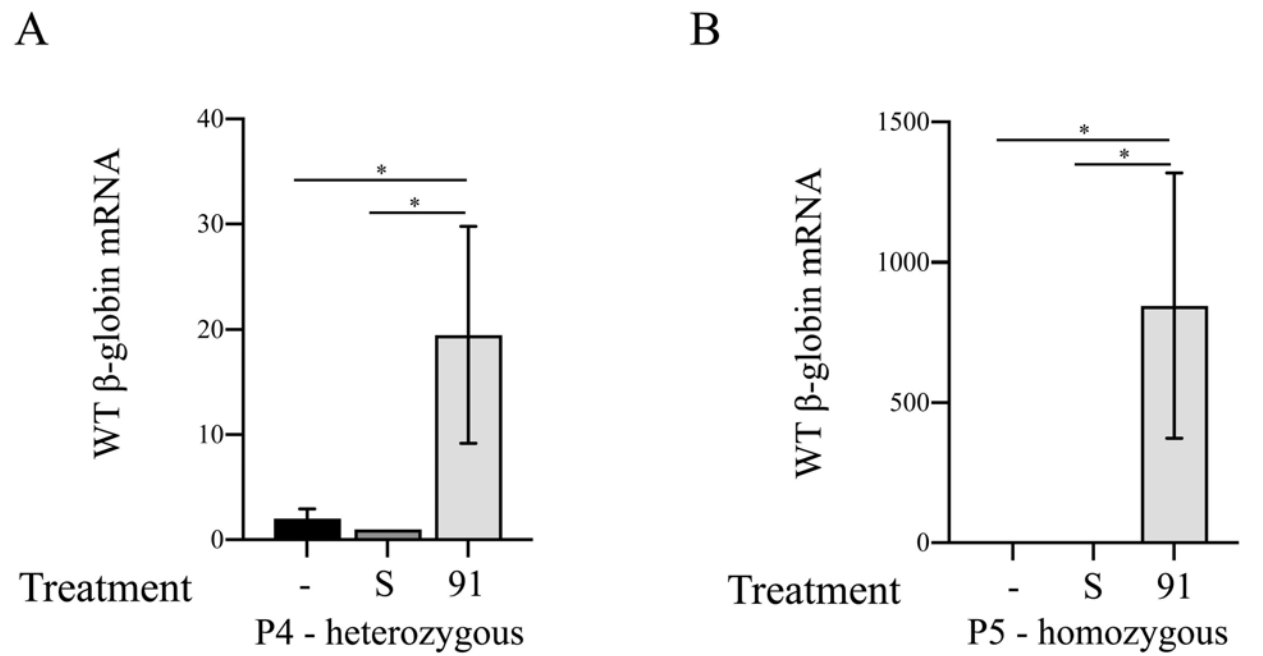
A
WT β-globin mRNA
40
30
20
10
0
*
*
Treatment
-
S
91
P4 - heterozygous
B
WT β-globin mRNA
1500
1000
500
0
*
*
Treatment
-
S
91
P5 - homozygous

Figure 8

A

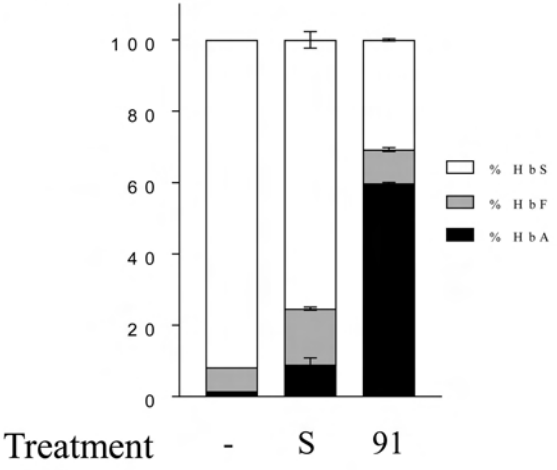

B

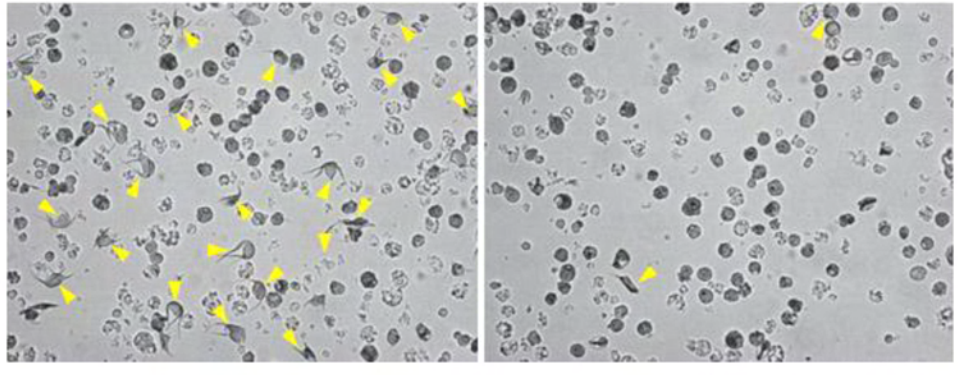

Supplementary methods

Statistics

For three or more groups, we compared means with a one-way ANOVA test (for samples with normal distributions and equal variances by the Shapiro-Wilks normality test) or medians with a non-parametric Kruskal-Wallis test. For two groups, we compared means with a t-test (for samples with normal distributions by the Shapiro-Wilks normality test) or medians with a Mann-Whitney test. All tests were done using GraphPad Prism software, version 7.

RNA, RT-PCR, and Quantitative PCR (Q-PCR)

Total RNA was isolated using Trizol (ThermoFisher). Retrotranscription of total mRNA was done using the SuperScript™ III First Strand Kit (ThermoFisher). PCR reactions were performed with the following primers: Fw: 5′-GGCAAGGTGAACGTGGATGAAGTT -3′; Rev: 5′-TAGGCAGAATCCAGATGCTCAAGG-3′. Sequencing on amplified products was completed by using the QIAquick Gel Extraction Kit, Qiagen) and cloned in TOPO® TA Cloning® Kits for Sequencing (Invitrogen, Carlsbad, CA). Q-PCR reactions were performed using the ABI 7900HT or Viia7 systems (Applied Biosystems), with either TaqMan (TaqMan PCR 2X Master Mix from ThermoFisher) or SYBR Green (Power SYBR from ThermoFisher or iTaqTM SYBR® Green Supermix from Bio-Rad) chemistry. Quantitative real-time PCR assays of globin, GAPDH, and glycophorin-A transcripts were carried out using gene-specific double fluorescently labeled probes. The following primer and probe sequences were used (forward, reverse and probe, when used, of each gene, respectively): WT correctly spliced β-globin primers = Fw: 5′-CACCTTTGCCACACTGAGTGA-3′; Rev: 5′-GCCCAG GAGCCTGAAGTTCT-3′; 5′-FAM-CACTGTGACAAGCTGCACGTGGATCC-IOWA BLACK-3′. The following TaqMan inventoried Gene Expression assays from Thermo Fisher were used: GAPDH: Hs02758991_g1; GYPA: Hs00266777_m1. Q-PCR results of WT β-globin were normalized by GAPDH to control for the total amount of cDNA and GYPA to control for the level of differentiation across samples. For PCR of human β-globin cDNA, the following primers were used: Fwd 5′-GTGCGAGAGCGTCAGTATTAAG-3′, Rev 5′-TCCCTGCTTGCCCATACTA-3′.

Droplet digital polymerase chain reactions (ddPCR)

Reactions were performed by Rain Drop plus Digital PCR system (RainDance Technologies). Droplets were generated using RainDance Source chips (RainDance Technologies) from 20 ng of cDNA and deposited in PCR tubes. PCR tubes were transferred into a thermocycler and processed using the following parameters: 10 min 95°C, then 45 cycles of 95°C for 15 sec, and 60°C for 1 min with a ramping speed of 0.6°C/sec, followed by 98°C for 10 min. After PCR completion, tubes were transferred into RainDance Sense chips (RainDance technologies) for fluorescence measurements. The RainDrop Analyst Software (RainDance technologies) was used to analyze the data set to define thresholds and count droplets. Endogenous cDNA amount was quantified by a primer/probe set against human β-actin gene (ThermoFisher Scientific). The wild type of β-globin assay sequences were as follows: 5′- CTGCACGTGGATCCTGAGAA -3′ (forward primer), 5′- GTGATGGGCCAGCACACA -3′ (reverse primer) and 5′-FAM- TTCAGGCTCCTGGGCA -MGBNFQ (probe) (Applied Biosystems).

Subsequent testing to measure the proportion of WT and IVS2-745 HBB (Supplementary Figure 6) were performed by Bio-Rad Droplet Digital PCR system, recently acquired by our laboratory. Droplets were prepared using Automated Droplet Generator (Biorad) from 22 ul of PCR mixture, followed by PCR reaction using C1000 Touch Thermal Cycler (Biorad) with the following parameters: 10 min 95°C, then 45 cycles of 95°C for 15 sec and 61°C for 2 min with a ramping speed of 1°C/sec, followed by 98°C for 10 min. Droplets fluorescence measurements were performed using QX200 Droplet Reader and QuantaSoft Software (Biorad). Minimum of 10000 drops were analyzed. Endogenous cDNA amount was quantified by a primer/probe set against human AHSP gene (Hs00372339_g1, ThermoFisher Scientific). The wild type HBB assay sequences were as follows: 5′- GAAGGCTCATGGCAAGAAAG -3′ (forward primer), 5′-CTGGTGGGGTGAATTCTTTG -3′ (reverse primer) and 5′-FAM- ACTTCAGGCTCCTGGGCAACGT -MGBNFQ (probe) (Biorad). The IVS2-745 HBB assay sequences were as follows: 5′- GAGAACTTCAGGGGCAATAATG -3′

(forward primer), 5′- AGCAATATGAAACCTCTTACATCAGT -3′ (reverse primer) and 5′-HEX-TCATGCCTCTTTGCACCATTCTAA -MGBNFQ (probe) (Biorad). The α-globin assay sequences were as follows:5'CGACAAGACCAACGTCAAGG – 3' (forward primer), 5'- ACAGGAACATCCTCTCCAGG-3' (reverse primer) and 5'- HEX-CACGCTGGCGAGTATGGTGC-MGBNFQ (probe) (Biorad).

Vector production and Titering

The human β-globin sequence was mutagenized with the IVS2-745 β-globin sequence, creating a lentiviral vector expressing human IVS2-745 β-globin. Viral stocks were generated by co-transfection into 293T cells (30). Viral supernatants were collected at 24 and 48 hours and filtered through cellulose acetate (0.2 μm). Following ultracentrifugation, serial dilutions of concentrated virus were used to infect 1e5 NIH 3T3 cells (ATCC, Manassas, VA) in 1 mL of transfection buffer complemented with polybrene (Millipore, Billerica, MA) at a final concentration of 8 μg/mL. Genomic DNA was extracted after 3 days using phenol-chloroform-isoamylic alcohol. The multiplicity of infection (MOI) was calculated using the following formula: number of cells (1e5) X dilution factor (1 mL/μL viral preparation) X VCN (measured via real-time PCR, using oligos for WPRE element and Transferrin Receptor gene, see copy number determination) (23).

Copy Number Determination

The number of integrations (VCN) was quantified by Q-PCR using Oligos for (Fw: 5′-GTGCGAGAGCGTCAGTATTAAG-3′; Rev: 5′-TCCCTGCTTGCCCATACTA-3′) for a specific sequence present in the vector (GAG) and compared it to an endogenous control present in two copies within the genome (mouse Transferrin=Fw: 5′-TGTTGTAGTAGGAGCCCAGAGAGA-3′; Rev:5′-AGACCTGTTCCCACACTGGACTT-3′; human ID-1 = Fw: 5′-AAGGTGAGCAAGGTGGAGATTC-3′; Rev: 5′-TTCCGAGTTCAGCTCCAACTG-3′).

Supplementary Table 1

Sequences of β-globin cDNA (WT and mutant 745)
Exons are indicated in different shades of orange. Intronic insertion of 165bp due to the mutation is indicated in green
Stop codon is highlighted in red

cDNA _ β-globin:

CGGCTGTCATCACTTAGACCTCACCCTGTGGAGCCACACCCTAGGGTTGGCCAATCTACTCCCAGGAGCAGG
GAGGGCAGGAGCCAGGGCTGGGCATAAAAGTCAGGGCAGAGCCATCTATTGCTTACATTTGCTTCTGACAC
AACTGTGTTCACTAGCAACCTCAAACAGACACCATGGTGCACCTGACTCCTGAGGAGAAGTCTGCCGTTACT
GCCCTGTGGGGCAAGGTGAACGTGGATGAAGTTGGTGGTGAGGCCCTGGGCAGGCTGCTGGTGGTCTACCC
TTGGACCCAGAGGTTCTTTGAGTCCTTTGGGGATCTGTCCACTCCTGATGCTGTTATGGGCAACCCTAAGGT
GAAGGCTCATGGCAAGAAAGTGCTCGGTGCCTTTAGTGATGGCCTGGCTCACCTGGACAACCTCAAGGGCA
CCTTTGCCACACTGAGTGAGCTGCACTGTGACAAGCTGCACGTGGATCCTGAGAACTTCAGGCTCCTGGGCA
ACGTGCTGGTCTGTGTGCTGGCCCATCACTTTGGCAAAGAATTCACCCCACCAGTGCAGGCTGCCTATCAGA
AAGTGGTGGCTGGTGTGGCTAATGCCCTGGCCCACAAGTATCACTAAGCTCGCTTTCTTGCTGTCCAATTTC
TATTAAAGGTTCCTTTGTTCCCTAAGTCCAACTACTAAACTGGGGGATATTATGAAGGGCCTTGAGCATCTG
GATTCTGCCTAATAAAAAACATTTATTTTCATTGCAA

Extra intron 165bp generated from aberrant splicing in IVS2-745 is a C→G mutation:

GGCAATAATGATACAATGTATCATGCCTCTTTGCACCATTCTAAAGAATAACAGTGATAATTTCTGGGTTAA
GGCAATAGCAATATTTCTGCATATAAATATTTCTGCATATAAATTGTAACTGATGTAAGAGGTTTCATATTG
CTAATAGCAGCTACAATCCAG

cDNA_ mutant β-globin 745:

CGGCTGTCATCACTTAGACCTCACCCTGTGGAGCCACACCCTAGGGTTGGCCAATCTACTCCCAGGAGCAGG
GAGGGCAGGAGCCAGGGCTGGGCATAAAAGTCAGGGCAGAGCCATCTATTGCTTACATTTGCTTCTGACAC
AACTGTGTTCACTAGCAACCTCAAACAGACACCATGGTGCACCTGACTCCTGAGGAGAAGTCTGCCGTTACT
GCCCTGTGGGGCAAGGTGAACGTGGATGAAGTTGGTGGTGAGGCCCTGGGCAGGCTGCTGGTGGTCTACCC
TTGGACCCAGAGGTTCTTTGAGTCCTTTGGGGATCTGTCCACTCCTGATGCTGTTATGGGCAACCCTAAGGT
GAAGGCTCATGGCAAGAAAGTGCTCGGTGCCTTTAGTGATGGCCTGGCTCACCTGGACAACCTCAAGGGCA
CCTTTGCCACACTGAGTGAGCTGCACTGTGACAAGCTGCACGTGGATCCTGAGAACTTCAGGGGCAATAAT
GATACAATGTATCATGCCTCTTTGCACCATTCTAAAGAATAACAGTGATAATTTCTGGGTTAAGGCAATAGC
AATATTTCTGCATATAAATATTTCTGCATATAAATTGTAACTGATGTAAGAGGTTTCATATTGCTAATAGCA
GCTACAATCCAGCTCCTGGGCAACGTGCTGGTCTGTGTGCTGGCCCATCACTTTGGCAAAGAATTCACCCCA
CCAGTGCAGGCTGCCTATCAGAAAGTGGTGGCTGGTGTGGCTAATGCCCTGGCCCACAAGTATCACTAAGC
TCGCTTTCTTGCTGTCCAATTTCTATTAAAGGTTCCTTTGTTCCCTAAGTCCAACTACTAAACTGGGGGATAT
TATGAAGGGCCTTGAGCATCTGGATTCTGCCTAATAAAAAACATTTATTTTCATTGCAA

cDNA_ β-globin SEQUENCED from M13For after TopoTA cloning (241bp 100%complementary):

GGCTCCATCTATAGGGGCGATTGAATTTAGCGGCCGCGAATTCGCCCTTCTCACCTGGACAACCTCAAGGGC
ACCTTTGCCACACTGAGTGAGCTGCACTGTGACAAGCTGCACGTGGATCCTGAGAACTTCAGGCTCCTGGGC
AACGTGCTGGTCTGTGTGCTGGCCCATCACTTTGGCAAAGAATTCACCCCACCAGTGCAGGCTGCCTATCAG
AAAGTGGTGGCTGGTGTGGCTAATGAAGGGCGAATTCGTTTAAACCTGCAGGACTAGTCCCTTTAGTGAGG
GTTAATTCTGAGCTTGGCGTAATCATGGTCATAGCTGTTTCCTGTGTGAAATTGTTATCCGCTCACAATTCCA
CACAACATACGAGCCGGAAGCATAAAGTGTAAAGCCTGGGGTGCCTAATGAGTGAGCTAACTCACATTAAT
TGCGTTGCGCTCACTGCCCGCTTTCCAGTCGGGAAACCTGTCGTGCCAGCTGCATTAATGAATCGGCCAACG
CGCGGGGAGAGGCGGTTTGCGTATTGGGCGCTCTTCCGCTTCCTCGCTCACTGACTCGCTGCGCTCGGTCGT
TCGGCTGCGGCGAGCGGTATCAGCTCACTCAAAGGCGGTAATACGGTTATCCACAGAATCAGGGGATAACG
CAGGAAAGAACATGTGAGCAAAAGGCCAGCAAAAGGCCAGGAACCGTAAAAAGGCCGCGTTGCTGGCGTT
TTTCCATAGGCTCCGCCCCCCTGACGAGCATCACAAAAATCGACGCTCAAGTCAGAGGTGGCGAAACCCGA

CAGGACTATAAAGATACCAGGCGTTTCCCCCTGGAAAGCTCCCTCGTGCGCTCTCCTGTTCCGACCCTGCCG
CTTACCGGATACCTGTCCGCCTTTCTCCCTTCGGGAAGCGTGCGCTTTCTCATAGCTCACGCTGTAGGTATCT
CAGTTCGGTGTAGGTCGTTCGCTCCAAGCTGGCTGTGTGCACGAACCCCCCCGTTCAGCCCGACGCTGCGCC
TATCCGGTAACTATCGTCTTGAGTCCAACCCGGGTAAGAACACCGACTTTATCCGCCCACCT

cDNA_ mutant β-globin 745 SEQUENCED from M13For after TopoTA cloning (405bp 100%complementary):

AGGATACATCTATAGGGCGATTGATTTAGCGGCCGCGAATTCGCCCTTCTCACCTGGACAACCTCAAGGGC
ACCTTTGCCACACTGAGTGAGCTGCACTGTGACAAGCTGCACGTGGATCCTGAGAACTTCAGGGGCAATAA
TGATACAATGTATCATGCCTCTTTGCACCATTCTAAAGAATAACAGTGATAATTTCTGGGTTAAGGCAATAG
CAATATCTCTGCATATAAATATTTCTGCATATAAATTGTAACTGATGTAAGAGGTTTCATATTGCTAATAGC
AGCTACAATCCAGCTCCTGGGCAACGTGCTGGTCTGTGTGCTGGCCCATCACTTTGGCAAAGAATTCACCCC
ACCAGTGCAGGCTGCCTATCAGAAAGTGGTGGCTGGTGTGGCTAATGAAGGGCGAATTCGTTTAAACCTGC
AGGACTAGTCCCTTTAGTGAGGGTTAATTCTGAGCTTGGCGTAATCATGGTCATAGCTGTTTCCTGTGTGAA
ATTGTTATCCGCTCACAATTCCACACAACATACGAGCCGGAAGCATAAAGTGTAAAGCCTGGGGTGCCTAA
TGAGTGAGCTAACTCACATTAATTGCGTTGCGCTCACTGCCCGCTTTCCAGTCGGGAAACCTGTCGTGCCAG
CTGCATTAATGAATCGGCCAACGCGCGGGGAGAGGCGGTTTGCGTATTGGGCGCTCTTCCGCTTCCTCGCTC
ACTGACTCGCTGCGCTCGGTCGTTCGGCTGCGGCGAGCGGTATCAGCTCACTCAAAGGCGGTAATACGGTT
ATCCACAGAATCAGGGGATAACGCAGGAAAGAACATGTGAGCAAAAGGCCAGCAAAAGGGCCAGGAACC
GTAAAAAGGCCGCGTTGCTGGCGTTTTTCCATAGGCTCCGCCCCCCTGACGAGCATCACAAAAATCGACGCT
CAAGTCAGAGGTGGCGAAACCCGACAGGACTATAAGATACCAGGCGTTTCCCCCTGTAGCTCCCTCGTGCG
CCTCCTCCTGTCCGACCCTGCCGCTACCGGATACCTGTCGCTTTCTCCGTCGGAGCGTGCGCTTTCTCATAGC
TCACGCTGTAGATTCTCAGTCGGTGTAGGTCGTCCGCTCCAGCTGGGCTGGGTGGTGACG

Supplementary Table 2

Sequences of 91-92-93 targeting the IVS2-745 HBB

ID	Sequence
91	CTTTAGAATGGTGCAAAG
92	TTCTTTAGAATGGTGCAA
93	TATTCTTTAGAATGGTGC

Supplementary Table 3

Schematic representation of SSO-target sites in the beta-globin gene

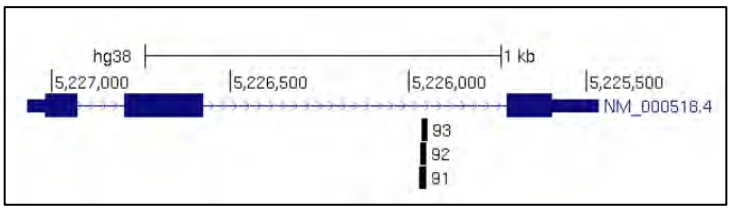

Supplementary Table 4

Results of search for TF binding sites on http://rbpdb.ccbr.utoronto.ca/
The red highlights areas the 3 ASOs bind while the underline marks the splicing factor binding sites

Sequence:

1 AGGGCAAUAA UGAUACAAUG UAUCAUGCCU CUUUGCACCA UUCUAAAGAA UAACAGUGAU

AAUUUCUGGG UUAAGGCAA

Score	Relative Score	RBP Name	Matching sequence
9.795457	81%	SNRPA	UUUGCACC
7.746982	96%	SNRPA	UUUGCAC
4.738923	92%	SFRS13A	AAAGAAU
4.652089	100%	KHDRBS3	AAUAAU
4.449274	95%	KHDRBS3	GAUAAU
4.09405	88%	KHDRBS3	UCUAAA
4.020734	86%	KHDRBS3	AAUAAC

Supplementary Figure 1. Splicing of WT human β-globin and aberrant splicing on mutant IVS2-745. IVS2-745 occurs in the intravenous sequence, or intron 2, of the beta-globin gene. It generates an aberrant 5' splice site at nucleotide 745 (indicated by the yellow circle). A corresponding cryptic 3' splice site at nucleotide 579 is activated, resulting in the inclusion of a 165nt sequence in the aberrant pre-mRNA. The IVS2-745 mRNA does not translate into functional beta-globin protein, given that the extra intronic sequence introduces a stop codon 48nt after exon 2.

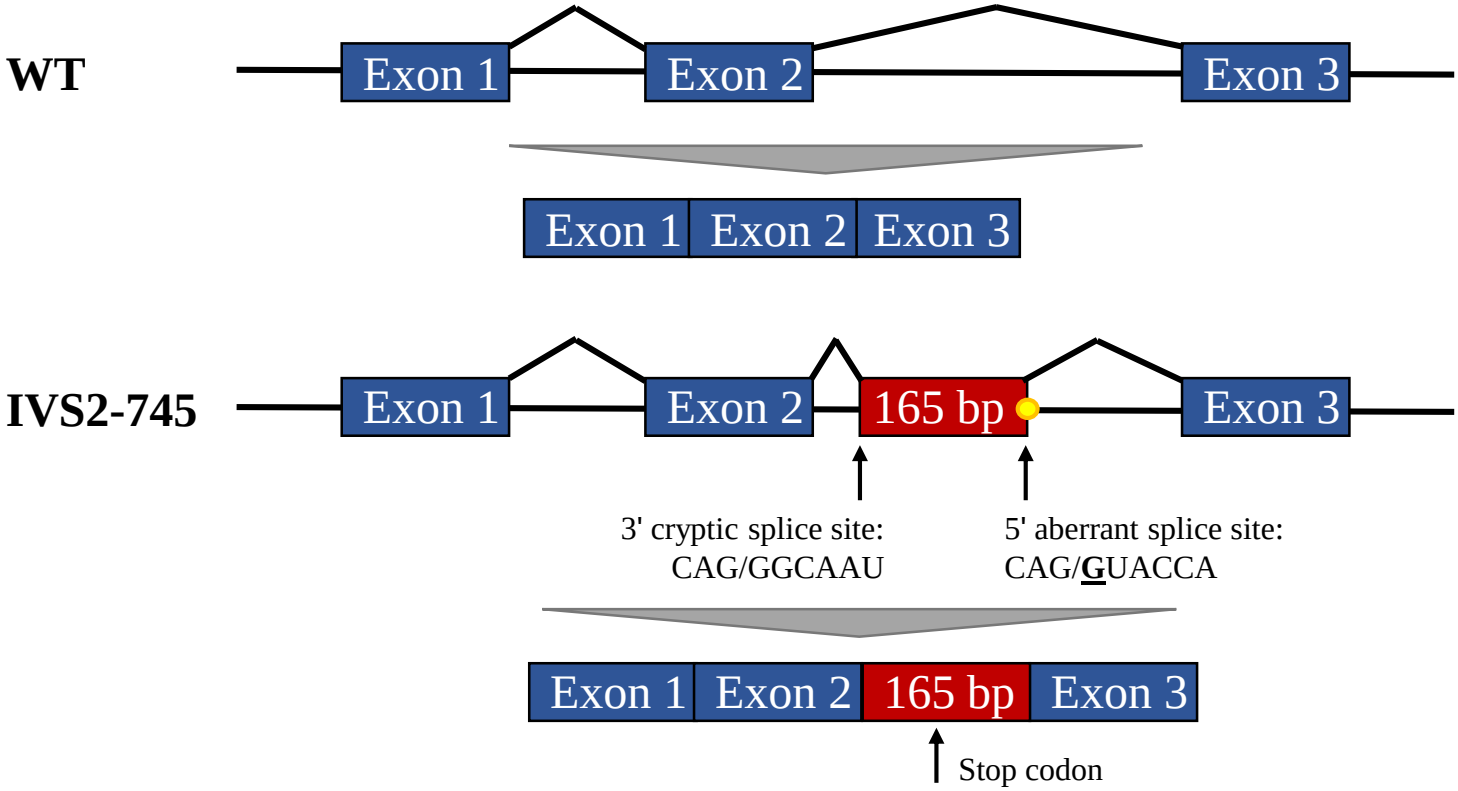

Supplementary Figure 2. Pre-screening of 2'-MOE-SSOs in mouse erythroleukemia (MEL) cells expressing the aberrant IVS2-745 HBB for splicing correction (A) The AnkCT9W lentivirus, which expresses wild-type beta-globin was modified with mutagenesis (yellow circle) to express the IVS2-745 beta-globin. (B) MEL-745 cells were created by infecting MEL cells with the AnkCT9W-745 lentivirus. C) Eleven 2' MOE-SSOs targeting the aberrant mRNA and a scramble dose (all 5μM) were originally tested for their ability to correct splicing in MEL cells expressing the aberrant IVS2-745 mRNA.

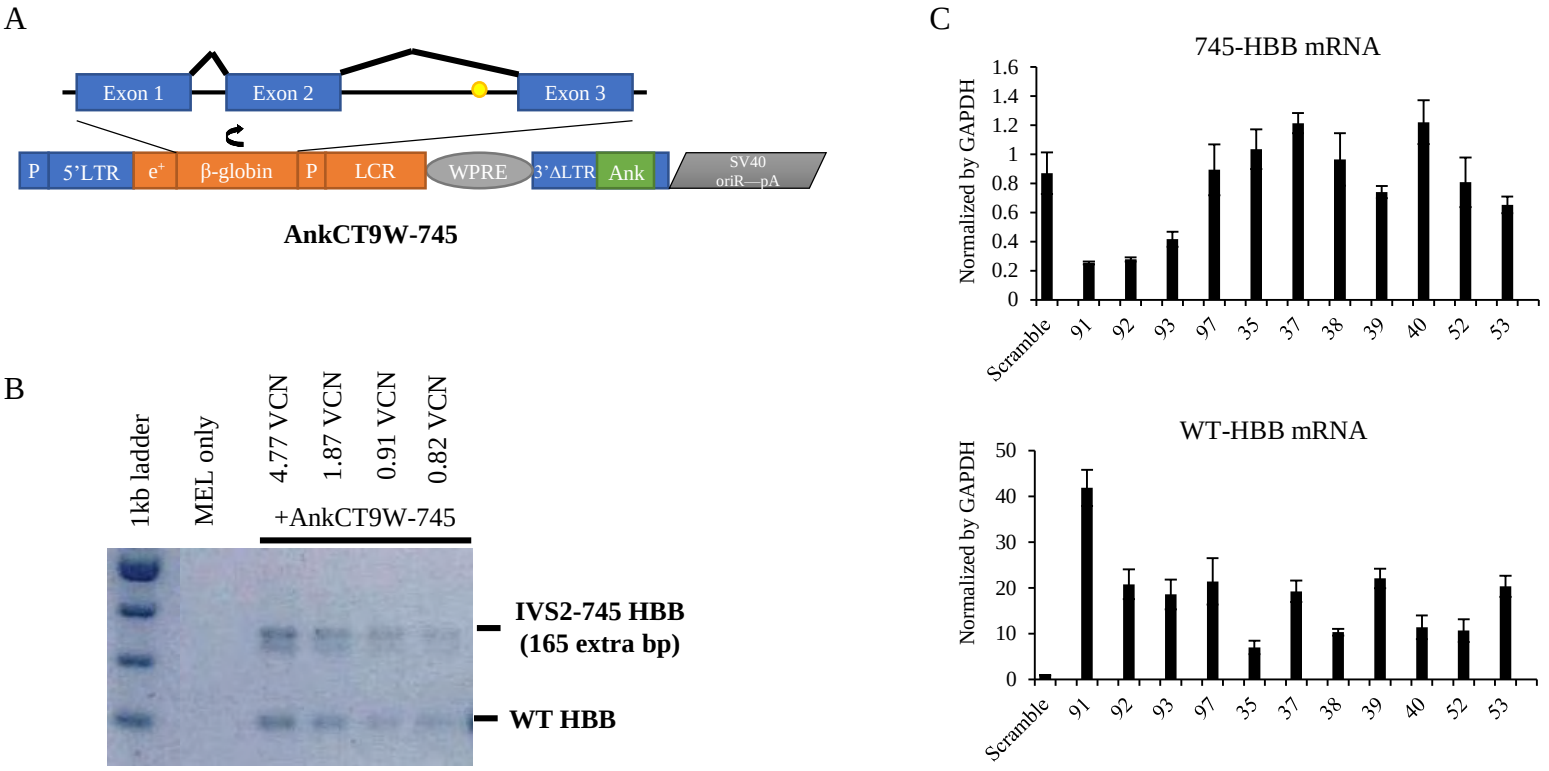

Supplementary Figure 3. Characterization of samples by flow cytometry at day-2, 5 and 8 of differentiation (in WT and IVS2-745 IVS1-6 specimen specimens). (A**)** Cell size and density is reduced throughout erythroid maturation, as indicated by reduction of SSC-FSC. As expected, (B) maturation of erythroid cells is accompanied by increased expression of the CD235a (GPA) marker and progressive reduction of CD71 in both WT and BT IVS2-745/ IVS1-6 cells. Maturation of erythroid cells is accompanied by decreased expression of CD117 (C), CD44 (D) and CD71 (E) markers and increased expression of the CD235a (GPA) (F). Accordingly, cell pellets become more red (G).

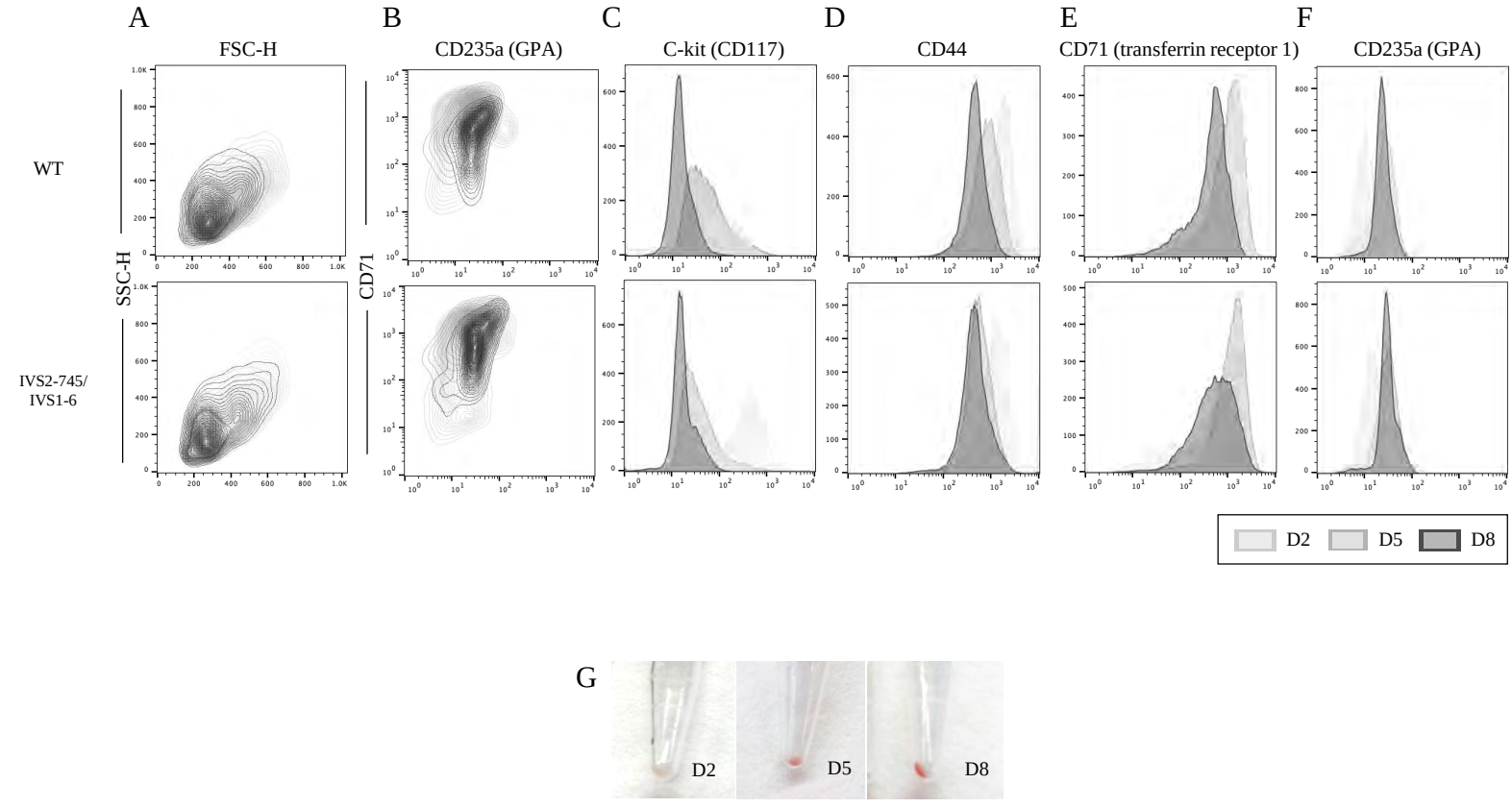

Supplementary Figure 4. Cell proliferation, mRNA and protein expression in WT and IVS2-745/IVS1-6 specimen specimens). (A) Cell proliferation and proportion of benzidine positive cell in erythroblasts isolated from healthy individual and from a patient with IVS1-6 / IVS2-745 BT, at different stages of erythroid maturation. (B) Abundance of WT beta-globin mRNA and (C) separation of tetrameric hemoglobins in specimens from A and (D) relative HbA proportion versus HbA absolute concentration calculated from C in 1E+06 benzidine positive cells collected at D8. ***p< 0.001, **** p< 0.0001.

A

WT

Day	Proliferation	Benzidine count
D2	1.4-fold	0.1%
D5	4.4-fold	83.1%
D8	10.2-fold	93.7%

IVS1-6 / IVS2-745

Day	Proliferation	Benzidine count
D2	0.9-fold	0.1%
D5	3.9-fold	97.2%
D8	12.1-fold	82%

B

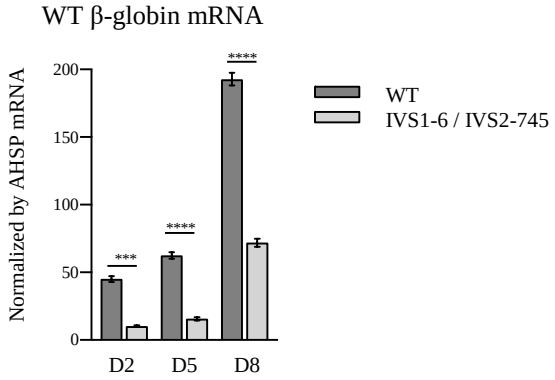

C

WT

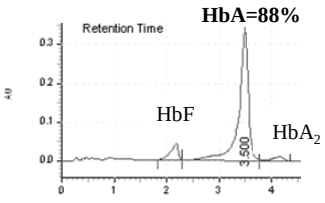

IVS1-6 / IVS2-745

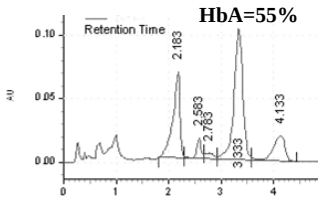

D

Proportion of HbA% in WT/BT specimen	Proportion of absolute HbA (area under curve) in WT/BT specimen
1.6-fold	3.35-fold

Supplementary Figure 5. Electrophoresis of PCR products of cDNA obtained from erythroblasts from patients with the IVS2-745 mutation. Bands relative to WT and aberrant IVS2-745 β-globin cDNA amplification of the two distinct messengers are indicated. (A) P1 specimen treated with scramble and with the 2'-MOE-SSOs 91, 92 and 93 at a 5μM dose. (B) P1 specimen treated with scramble and with the same oligos at a 5μM and a 25μM dose. (C) and (D) Specimen P3 and P4 treated with scramble and with the three 2'-MOE-SSOs at a 50μM dose.

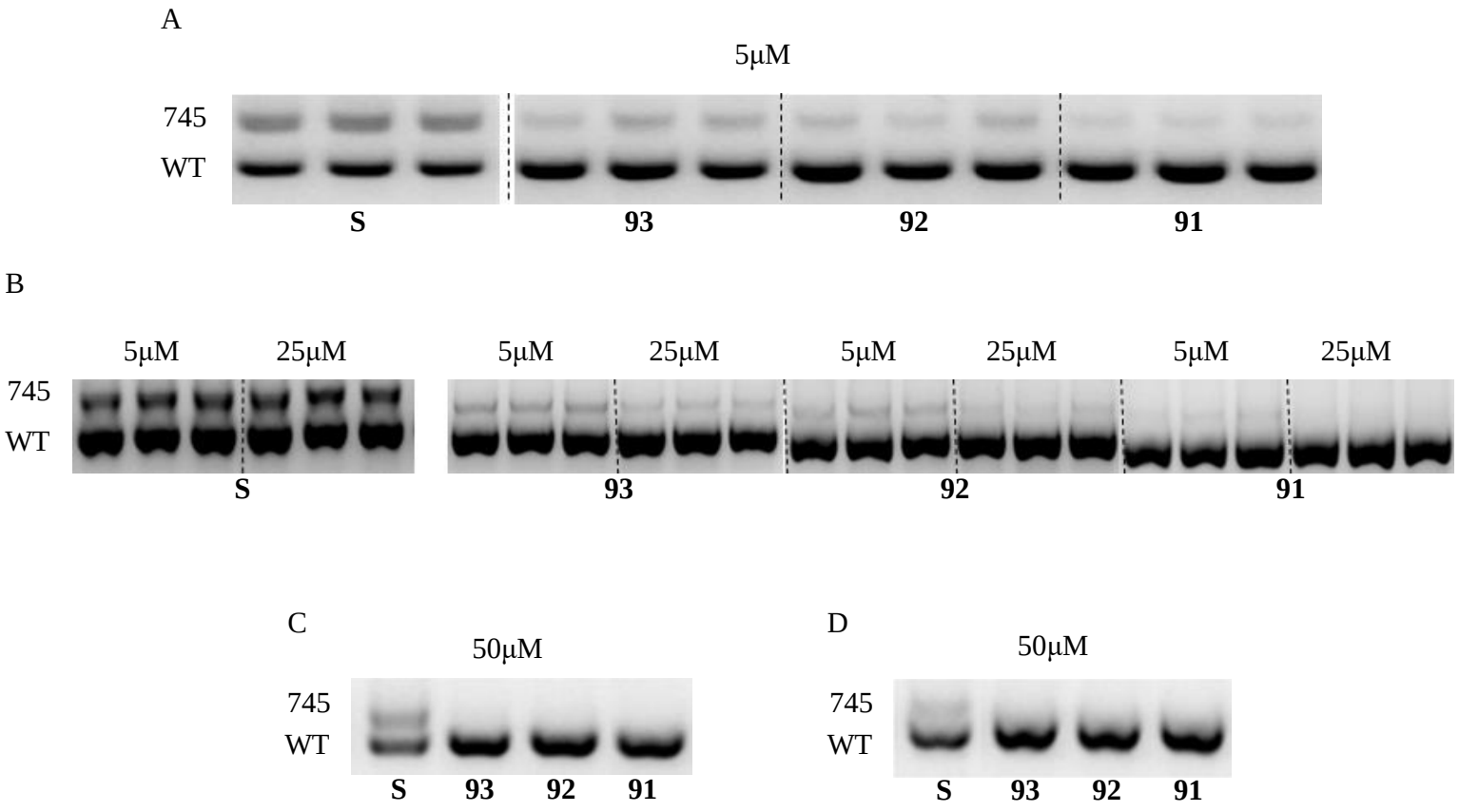

Supplementary Figure 6. 2'-MOE-SSOs 91 greatly increases amount of WT over IVS2-745 β-globin mRNA. In the ddPCR analysis in A), y axes indicates relative expression of WT β-globin normalized to the IVS2-745, while in B) the cDNA concentration in the generated droplets of the same sample analyzed with WT or the IVS2-745 probe and primer sets. IVS-2-745/β0 heterozygous sample, P4. Statistics (ANOVA/Kruskal-Wallis) compared scramble control and non-treated sample to 2'-MOE-SSO 91 treatment were at the dose of 50μM. n=3. **** p< 0.0001. In B) statistic indicated by * represent the different WT mRNA abundance while # represent the different IVS2-745 mRNA abundance.